ICARUS 38, 288–299 (1979)

Mariner 9 Ultraviolet Spectrometer Experiment: Vertical Distribution of Ozone on Mars

W. M. WEHRBEIN,[1] C. W. HORD, AND C. A. BARTH

Department of Astro-Geophysics and Laboratory for Atmospheric and Space Physics, University of Colorado, Boulder, Colorado 80309

Received October 11, 1978; revised December 7, 1978

The vertical distribution of ozone in the atmosphere of Mars is computed from ultraviolet spectra obtained by the Mariner 9 spacecraft. In the Northern Hemisphere the ozone scale height is much smaller than the atmospheric scale height in midlatitudes and increases rapidly to a maximum farther north. At high latitudes (above 60°) there is no significant difference between the scale heights of ozone in the Northern (winter) Hemisphere and the Southern (summer) Hemisphere. Comparison of the ozone distribution with atmospheric temperature structure indicates that at some locations in the North, the density of water vapor increases with altitude, and the time for vertical mixing is about 3 days or more.

INTRODUCTION

Ozone was discovered on Mars by the ultraviolet spectrometer on Mariner 7 (Barth and Hord, 1971). About 10 μ-atm (1 μ-atm is a column abundance of 2.689×10^{15} molecules cm^{-2}) of ozone was detected over the South Polar Cap during early spring in that hemisphere. From these observations it was not possible to ascertain whether ozone was an atmospheric constituent, was adsorbed on solid carbon dioxide lying on the surface, or was adsorbed on finely divided carbon dioxide crystals suspended in the planetary atmosphere (Broida *et al.*, 1970).

Extensive investigations of the variations of ozone with season and latitude were accomplished with the Mariner 9 spacecraft, which provided observations of the planet for nearly half a Martian year. Asymmetries in ozone observations between North and South polar caps indicated that ozone is an atmospheric constituent (Lane *et al.*, 1973). The seasonal variations, described by Barth *et al.* (1973), were as follows. In early summer no ozone was seen. Ozone appeared in late summer and early fall over the polar cap and in association with the polar hood. By the end of summer, ozone amounts had increased from below the detectable limit of 3 μ-atm to more than 10 μ-atm. As the season progressed, ozone continued to increase, reaching a maximum from latitude 45° poleward during midwinter. In the North the maximum observed was 60 μ-atm; in the South the maximum was at least 30 μ-atm. Ozone amounts then began to decrease slowly, disappearing below the detectable limit in early summer.

INSTRUMENT

The ultraviolet spectrometer has been described in detail elsewhere (Hord *et al.*, 1970). The instrument scanned from 2100

[1] Present address: Department of Atmospheric Sciences, AK-40, University of Washington, Seattle, Wash. 98195.

0019-1035/79/050288-12$02.00/0

to 3500 Å in one of its two spectral channels every 3 sec with a spectral resolution of 15 Å. At the mean altitude of 2300 km, where many of the measurements were made, the effective field of view projected onto the planetary surface was approximately 30 by 10 km. Before analysis each spectrum was filtered to remove spurious data points, then compared to the solar flux spectrum and shifted slightly in wavelength in order to compensate for any systematic shift in the wavelength calibration of the spectrometer.

ATMOSPHERIC MODEL

The atmosphere of Mars is approximated as plane parallel, although Chapman functions are used to compute slant paths. The atmosphere is sufficiently thin that multiple-scattering effects may be neglected (Hord *et al.*, 1974). By composition the atmosphere is divided into two species: ozone, and constituents which are not ozone, called the continuum. Scattering by the continuum is assumed to be conservative, to follow the Rayleigh phase law, and to depend on some inverse power of wavelength. Extinction of radiation by the continuum is assumed negligible compared to extinction by ozone. Reflection by the lower boundary is described with an albedo independent of wavelength.

It is customary to refer to the reflectance R_λ of a planet, where

$$R_\lambda = 4\pi I_\lambda(0)/4\pi F_\lambda, \tag{1}$$

$I_\lambda(0)$ is the scattered radiation intensity, and πF_λ is the solar flux, both measured at the top of the planet's atmosphere. The expression for R_λ appropriate to the above atmospheric model is

$$R_\lambda = A\mu_0 \exp\{-[\bar{\tau}\beta(k;\lambda) + \tau_o\alpha(\lambda)]M\} + \frac{\bar{\tau}\beta(k;\lambda)p(\psi)}{4\mu}\int_0^1 \exp\{-[\bar{\tau}t\beta(k;\lambda) + \tau_o x(t)\alpha(\lambda)]M\}dt, \tag{2}$$

where A is the surface albedo, μ_0 is the cosine of the solar zenith angle, $\bar{\tau}$ is the total optical depth of the continuum at 3050 Å, $\beta(k;\lambda) = \bar{\tau}(\lambda)/\bar{\tau}(3050\text{ Å})$, τ_o is the total optical depth of ozone at 2550 Å, $\alpha(\lambda) = \tau_o(\lambda)/\tau_o(2550\text{ Å})$, M is the air-mass factor $1/\mu + 1/\mu_0$, $p(\psi)/4\pi$ is the phase function for scattering angle ψ, μ is the cosine of the spacecraft viewing angle, and $x(t)$ is the fraction of the column abundance of ozone lying above vertical optical depth coordinate t. Because many observations were made at large solar zenith or viewing angles, the reciprocal of the Chapman function has been used in place of the cosine for both μ and μ_0. Parameter k describes the wavelength dependence of the scattering coefficient and is defined by

$$\beta(k;\lambda) = (3050\text{ Å}/\lambda)^k. \tag{3}$$

MATHEMATICAL METHOD

Mariner 9 investigations of ozone on Mars have utilized a modeling method (e.g., Conrath, 1969) in which the distribution of ozone in the atmosphere is described with mathematical functions of a few parameters. In prior studies (e.g., Barth *et al.*, 1973) ozone was assumed to be mixed throughout the atmosphere, while scattering was assumed isotropic (i.e., $p(\psi) = 1$), and surface reflection was ignored for spectra obtained over the polar hood. For a homogeneous atmosphere, $x(t) = t$. The geometrical factors μ, μ_0, and M are known, so that in Eq. (2) reflectance R_λ is a function only of the variables $\bar{\tau}$ and k, which describe the continuum, and τ_o, which describes the ozone distribution.

These three variables were varied in order to achieve a least-squares fit between the reflectance data and the reflectance given by the model in the spectral range 2550 to 3500 Å. Data at wavelengths less than 2550 Å were not used because of their more unfavorable signal-to-noise ratio. One particular reflectance spectrum from

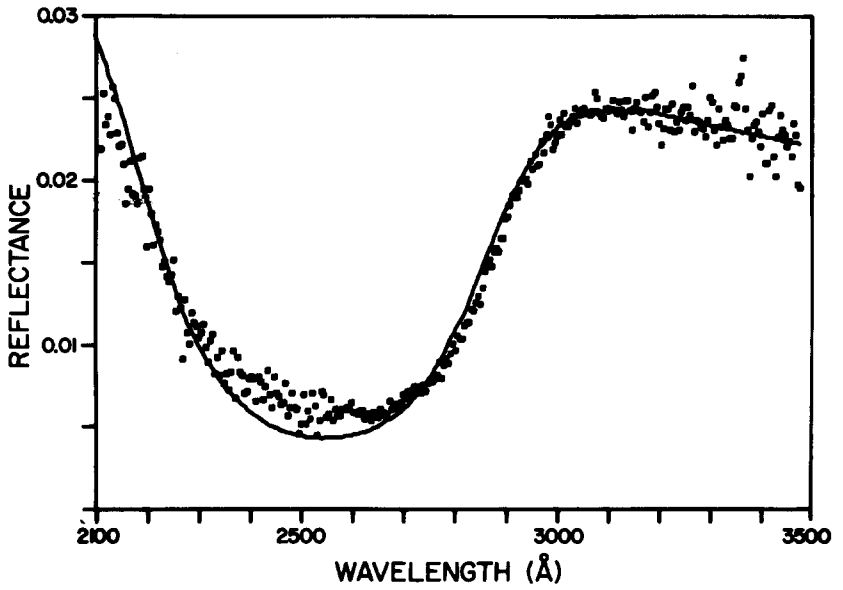

FIG. 1. Spectrum for DAS (data acquisition sequence time) 9270775 from orbit 214 (29 February 1972). Solid line is best fit to these data using the homogeneous model, fitted from λ = 2552 Å to λ = 3493 Å.

orbit 214 and the best fit using the homogeneous atmosphere model are shown in Fig. 1. Although this simple model reproduces the general shape of the Hartley absorption band of ozone seen in the data, it fails to match the details of the feature, particularly near the absorption maximum.

For the model utilized in the present study, reflection from the lower boundary is not neglected, and the angular distribu-

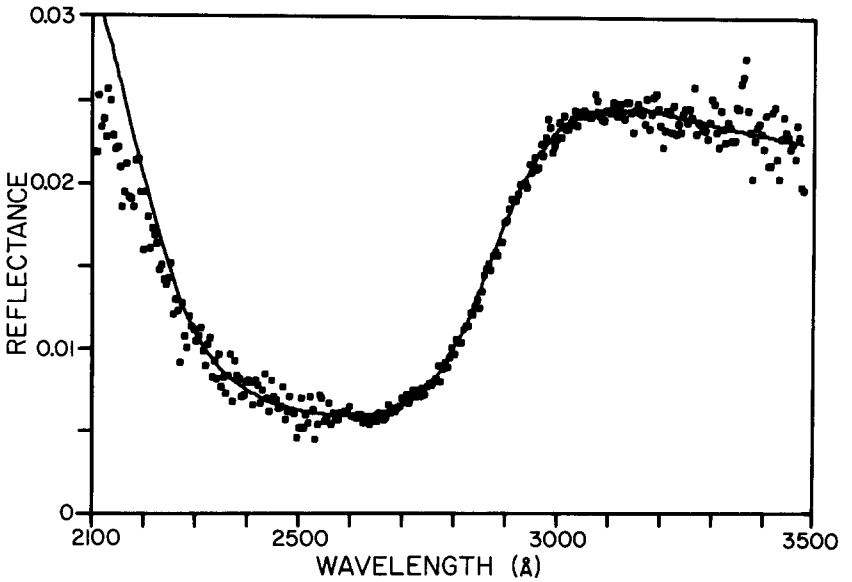

FIG. 2. Spectrum for DAS 9270775 from orbit 214. Solid line is best fit to these data using constant scale height model, fitted from λ = 2552 Å to λ = 3493 Å.

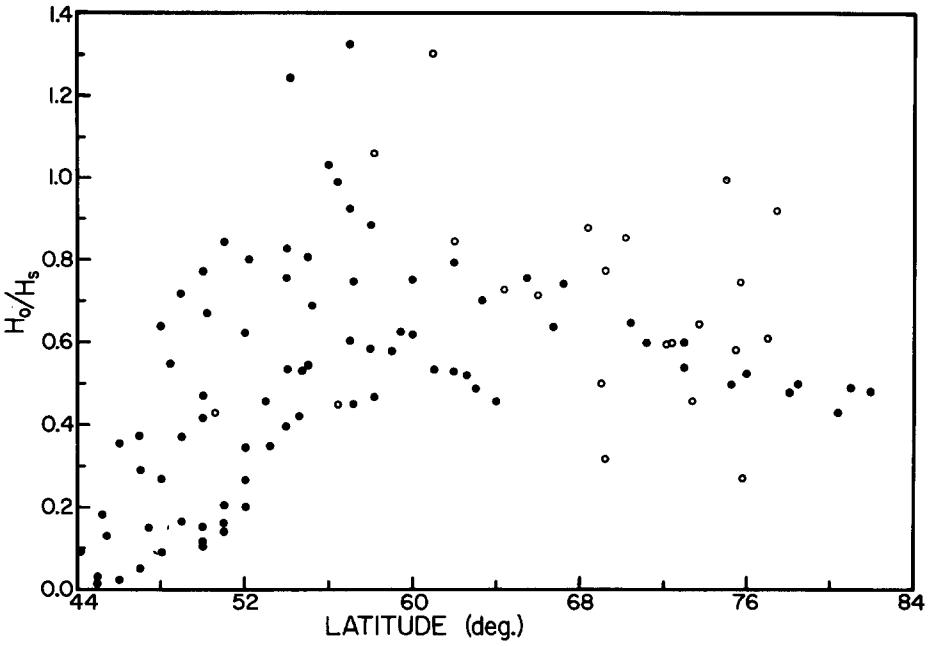

FIG. 3. Composite of H_o/H_s vs latitude. Solid dots represent Northern Hemisphere spectra, while open dots represent spectra from the Southern Hemisphere.

tion of scattered radiation is assumed to follow the Rayleigh law. Ozone is assumed to be distributed with a constant scale height H_o which may be different from the scale height of the continuum H_s. This model for ozone distribution is based on the calculated ozone profiles of Davis (1976), who used the photochemical theories of McElroy and Donahue (1972) and Parkinson and Hunten (1972). Each of these computed profiles displays a nearly constant scale height from the surface to about 10 or 20 km. About nine-tenths of the total atmospheric ozone resides below this level.

There are now five variables: albedo A describes the lower boundary, $\bar{\tau}$ and k describe the continuum, and τ_o and H_o/H_s describe the ozone distribution. If the lower boundary consists of optically thick clouds, then the model applies to the atmosphere above the cloud deck. Following Mateer's (1965) analysis of the information content of Umkehr measurements, it has been shown (Wehrbein, 1977) that there are no more than four or five independent pieces of information in the best of the Mariner 9 ultraviolet spectra. Therefore, five variables cannot be determined in a least-squares sense. Adapting the method developed by Twomey (1963, 1965) one finds solutions for the set of unknown parameters assuming "preconceived notion" values given by $\bar{\tau} = 0.03$, $k = 4$ (i.e., a clear atmosphere), $A = 0.0175$ (cf. Hord *et al.*, 1974), $\tau_o = 0.25$, and $H_o/H_s = 0.5$. (The scale height H_s of an isothermal carbon dioxide atmosphere at 200°K is 10 km.) The details of the mathematical solution are given in the Appendix. Figure 2 shows the reflectance spectrum displayed in Fig. 1 and the fit accomplished with this five-parameter model.

RESULTS

A total of 103 spectra were analyzed. Only 22 spectra obtained in the Southern Hemisphere have been considered, due to

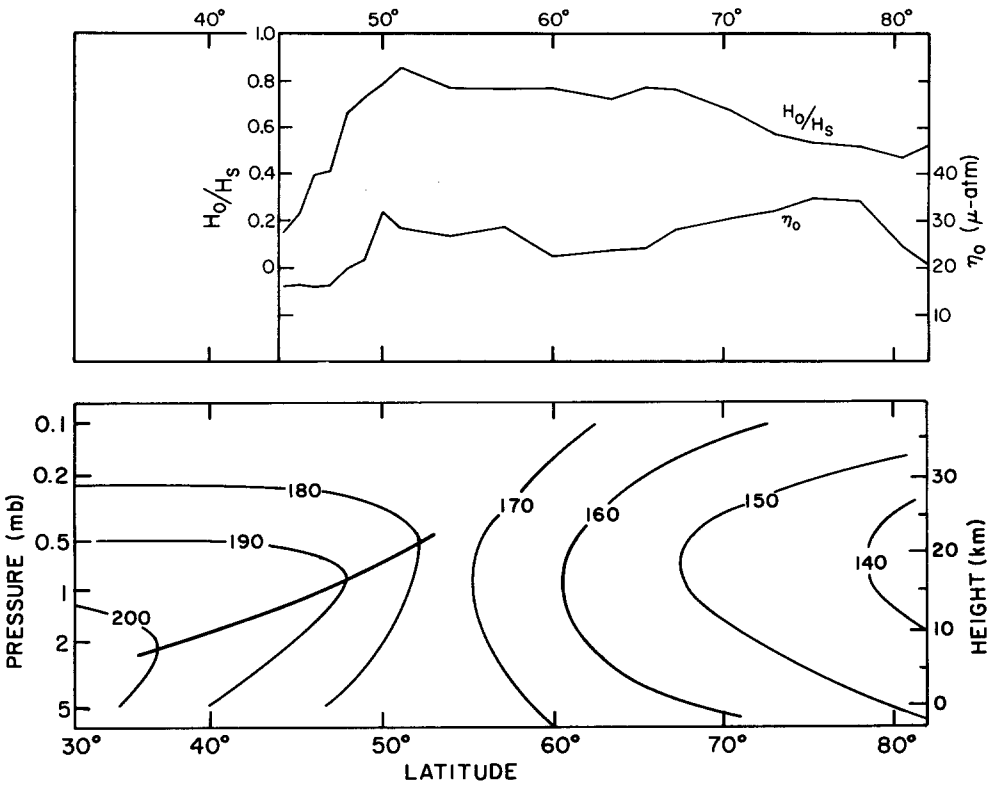

FIG. 4. Top part of figure is the ozone distribution in the Northern Hemisphere for orbit 202 (23 February 1972). Upper line is the scale height ratio H_o/H_s (scale on left). Lower line is the ozone column abundance in μ-atm (scale on right). Bottom part of figure is the temperature structure of the atmosphere from IRIS data. Heavy line indicates top of inversion layer.

the very small amounts of ozone present in that hemisphere during the season of observation (late summer). Two orbits in the Northern Hemisphere from midlatitudes to above 80°N have been investigated intensively. The development and variations in ozone distributions for 3 consecutive days in the same locality have also been investigated. All of the spectra chosen for study were obtained between orbits 180 and 220, which occurred from 12 February to 3 March 1972. This corresponds to the period a few days before vernal equinox in the Northern Hemisphere.

Comparison of Northern (Winter) and Southern (Summer) Hemispheres

Figure 3 shows the values of H_o/H_s for a composite of many spectra from several southern passes compared with a similar composite of many spectra from several northern passes. During this season (southern summer) ozone is rarely detected as far from the South Pole as southern midlatitudes, so almost all the southern spectra lie poleward of 60°S. For the 18 southern spectra south of 61°S, the average scale height ratio H_o/H_s is 0.67 with a standard deviation of 0.20. For the 20 northern spectra north of 61°N, the average value of H_o/H_s is 0.57 with a standard deviation of 0.11. Therefore, there is no significant difference in scale height ratio between Northern and Southern Hemispheres in the regions in both hemispheres where ozone is seen.

Latitude Dependence in the Northern Hemisphere

Ozone column abundance and scale height are plotted as a function of latitude along orbit 202 in the upper part of Fig. 4. The corresponding temperature structure in the lower part of the figure was constructed from Mariner 9 infrared interferometer spectrometer (IRIS) data (Conrath, private communication).

The scale height of the ozone distribution is small at onset, but increases rapidly to a maximum at about 51°N. This indicates that most of the ozone is confined to the part of the atmosphere below the temperature inversion layer. From about 50 to 68°N the scale height ratio is relatively constant at about 0.75. Poleward of 64°, H_o/H_s decreases to about 0.4 or 0.5 at 80°.

The ozone column abundance, after reaching a relative maximum at about 50°N, declines slightly to a relative minimum between 60 and 64°N. The ozone amount increases again to an absolute maximum at about 75°N, then decreases to 82°N. The smaller amount of ozone in very high latitudes may result from the lower production rate of odd oxygen in polar regions due to the greater attenuation of photodissociating radiation at large solar zenith angles. Alternatively, this feature may simply be an artificial result of the observational method. The air-mass factors at high latitudes are quite large, so that even in the far wings of the ozone absorption band, attenuation by the continuum will prevent the spectrometer from "seeing" all the way to the surface. Some ozone in the lower atmosphere may be hidden from view.

Ozone amounts and scale heights for orbit 186 are shown in the upper part of

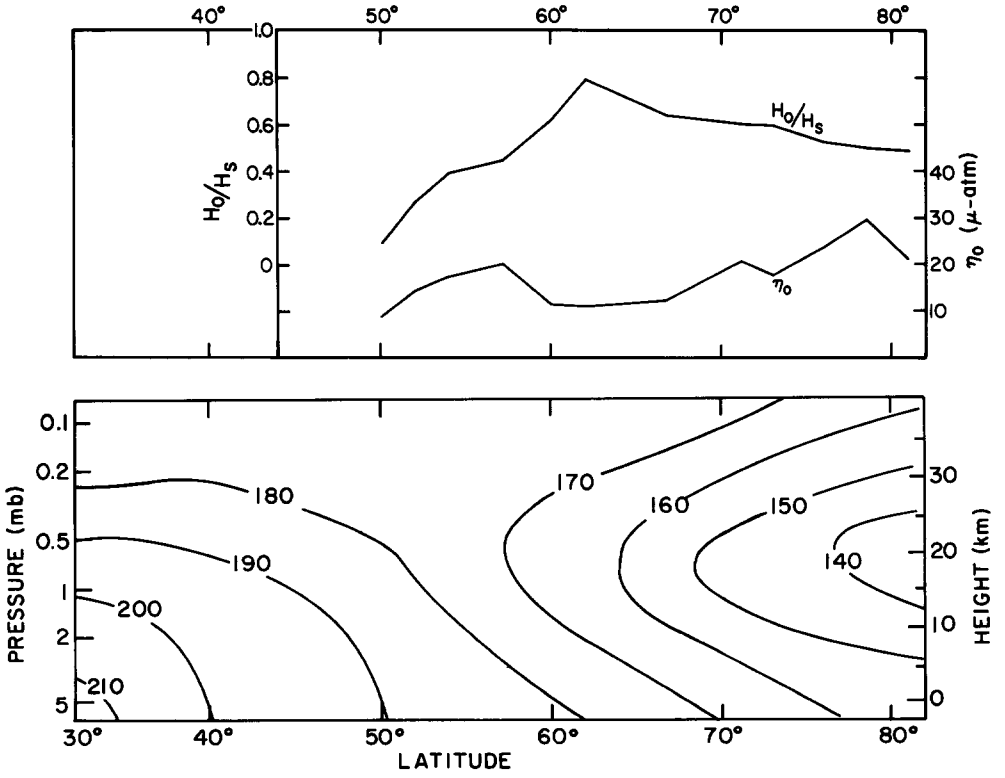

FIG. 5. Same as Fig. 4 for orbit 186 (15 February 1972).

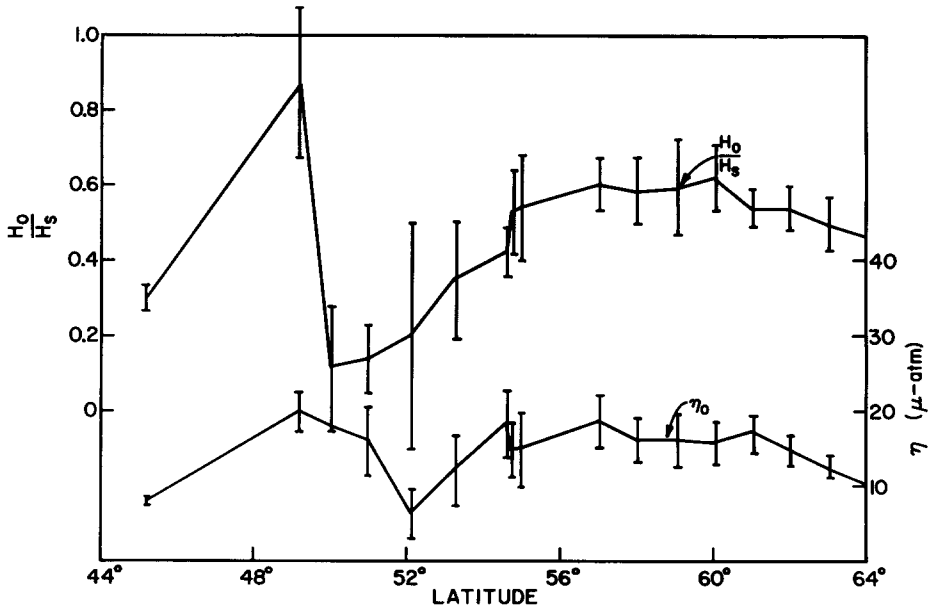

FIG. 6. Ozone distribution in the Northern Hemisphere for orbit 212 (28 February 1972). Error bars represent statistical error only.

Fig. 5. The temperature structure is presented in the lower part of the same figure. On orbit 186 the lower atmosphere was warmer than on orbit 202, and there is less ozone along orbit 186 at each corresponding latitude.

The extremely small scale heights observed at the point of ozone onset reveals

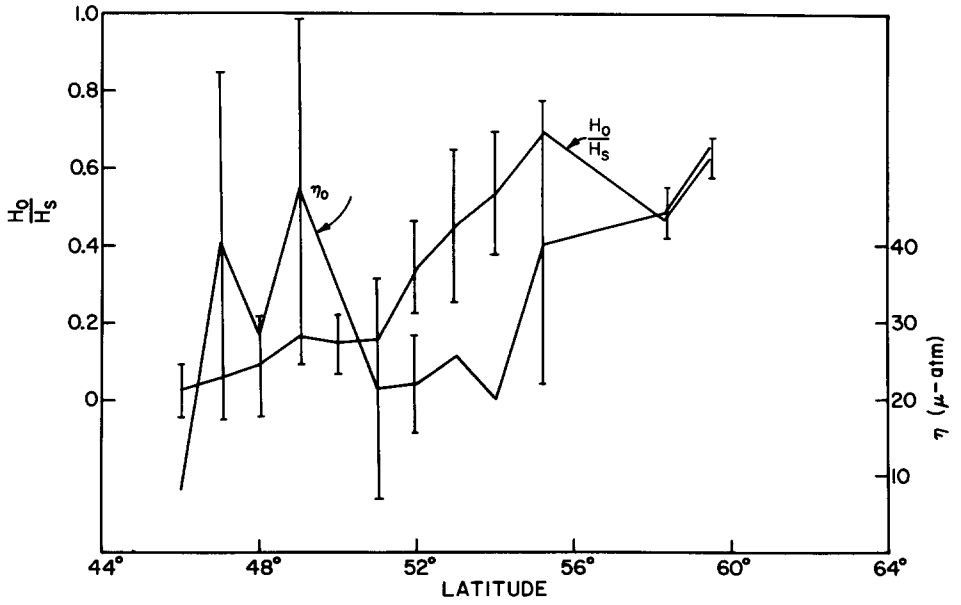

FIG. 7. Ozone distribution in the Northern Hemisphere for orbit 214 (29 February 1972). Some error bars are omitted for clarity.

two significant facts about the atmosphere at that location. First, vertical mixing in the lower atmosphere occurs on a time scale of a few days or more; and second, more water vapor is present at an altitude of a few kilometers than at the surface. These conclusions are reached by the following arguments. According to the photochemical theories (McElroy and Donahue, 1972; Parkinson and Hunten, 1972) the density of ozone is determined by the local density of odd hydrogen (H, OH, and HO_2). If odd hydrogen were mixed in the atmosphere, then the ozone distribution would depend only on the column abundance of water vapor in the atmosphere, not its vertical distribution. Furthermore, the ozone profiles of Davis (1976), computed with an eddy diffusion coefficient corresponding to a mixing time of about 9 hr, show that the ozone scale height varies little from the dry cases with abundant ozone to damper cases with very little ozone.

The observed ozone distribution at onset can be explained by postulating larger amounts of odd hydrogen at an altitude of a few kilometers than at the surface, therefore reducing the pool of odd oxygen (O and O_3) at this altitude. This argument suggests that odd hydrogen is not mixed; hence, the mixing time is comparable or longer than the midlatitude odd hydrogen lifetime of 3 days (Wehrbein, 1977). The high static stability of the atmosphere in both these locations is responsible for the slow vertical mixing.

The higher densities of odd hydrogen a few kilometers above the surface must be due to higher water vapor densities at

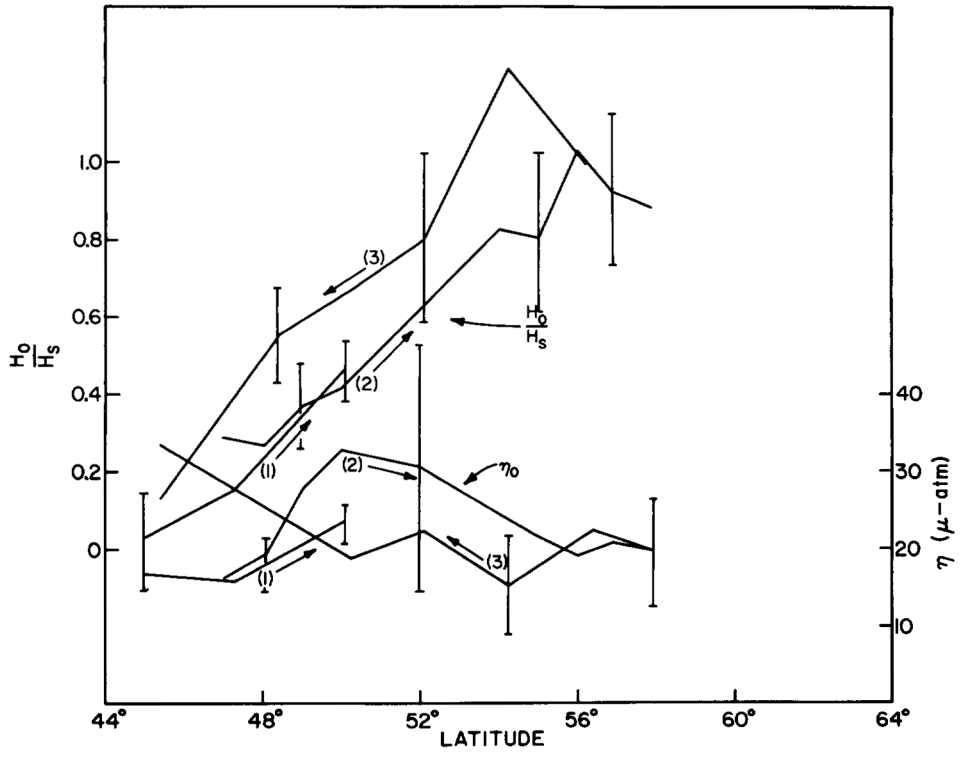

FIG. 8. Ozone distribution in the Northern Hemisphere for orbit 216 (1 March 1972). Numbers in parentheses refer to parts of orbit 216 delineated in Fig. 9. Arrows show direction of spacecraft motion. Some error bars are omitted for clarity.

the same altitude. Why the water vapor density should increase with altitude is problematical. Perhaps at the top of the inversion layer there is some entrainment of warmer, moister air from the layer lying above it. These cases may represent the dynamical interactions of two air masses with different origins and characteristics.

Ozone Variations From Day to Day

The variation in ozone and its correlation with cloud cover for 3 consecutive days in the same locality were investigated by Barth and Dick (1974). They used the homogeneous model of the atmosphere described earlier to determine ozone amounts. In the present work the same data have been analyzed with the constant scale height model. The results are shown in Figs. 6, 7, and 8. The corresponding TV images are found in Fig. 9.

The ozone scale height displays the same characteristics of small values at onset, a midlatitude plateau, and high-latitude decrease that were observed on orbits 202 and 186. Between the first and second days, atmospheric conditions changed considerably. An extensive and complicated system of wave clouds extended from about 42 to 60°N. Overlying this pattern from 45 to 60°N is a pattern of optically thick clouds formed by a flow from a different direction. Copious amounts of ozone are observed at quite low latitudes, and the maximum of 53 μ-atm at 59.5°N is more than 3 times the maximum of the preceding day.

By orbit 216 the large active wave cloud seen the previous day has been replaced by a diffuse cloud field in the far north and very thin low-level wavelets between 47 and 52°N. The field of view of the spacecraft on this orbit took a complicated route over the Martian surface traversing several latitude zones more than once. Three overlapping sections of this pass are plotted in Fig. 8. The ozone scale height for the first and second parts of this path is quite consistent. The third part has the same shape, but at larger values of H_o/H_s. Ozone column abundance varies even more among the three overlapping paths. Examination of television pictures reveals no clear differences between these paths. Apparently, some variation in the atmosphere, not revealed by the cloud cover, is responsible.

It appears that the extensive cloud system is related in some way to the large increase in ozone between the first and second days. A cold air mass moving in from the west containing less water vapor, less odd hydrogen, and consequently more ozone, could explain both the changes in cloud morphology and ozone abundance.

By the third day the cold air mass has passed and atmospheric conditions have nearly returned to those of 2 days earlier. However, there appears to be a rather slow southward drift to the ozone distribution. The onsets of ozone for the 3 days were seen at 49, 45, and, finally, 43°N. The scale height distribution shifts about 1 degree of latitude between the first and second days, and about 3 to 5 degrees southward between the second and third days. This corresponds to a southward displacement of about 30 to 50 km per day.

DISCUSSION

The distribution of ozone in the Martian atmosphere depends on atmospheric temperature. The local atmospheric temperature determines the maximum local water vapor density, water vapor density sets the odd hydrogen density, and odd hydrogen density determines the density of odd oxygen. In midlatitudes in the spring, strong atmospheric temperature inversions are typical and ozone is most abundant in the cold air near the surface, which is presumably drier than the warmer air lying above. Around the poles of either hemisphere the atmosphere is so cold that molecular hydrogen, rather than water

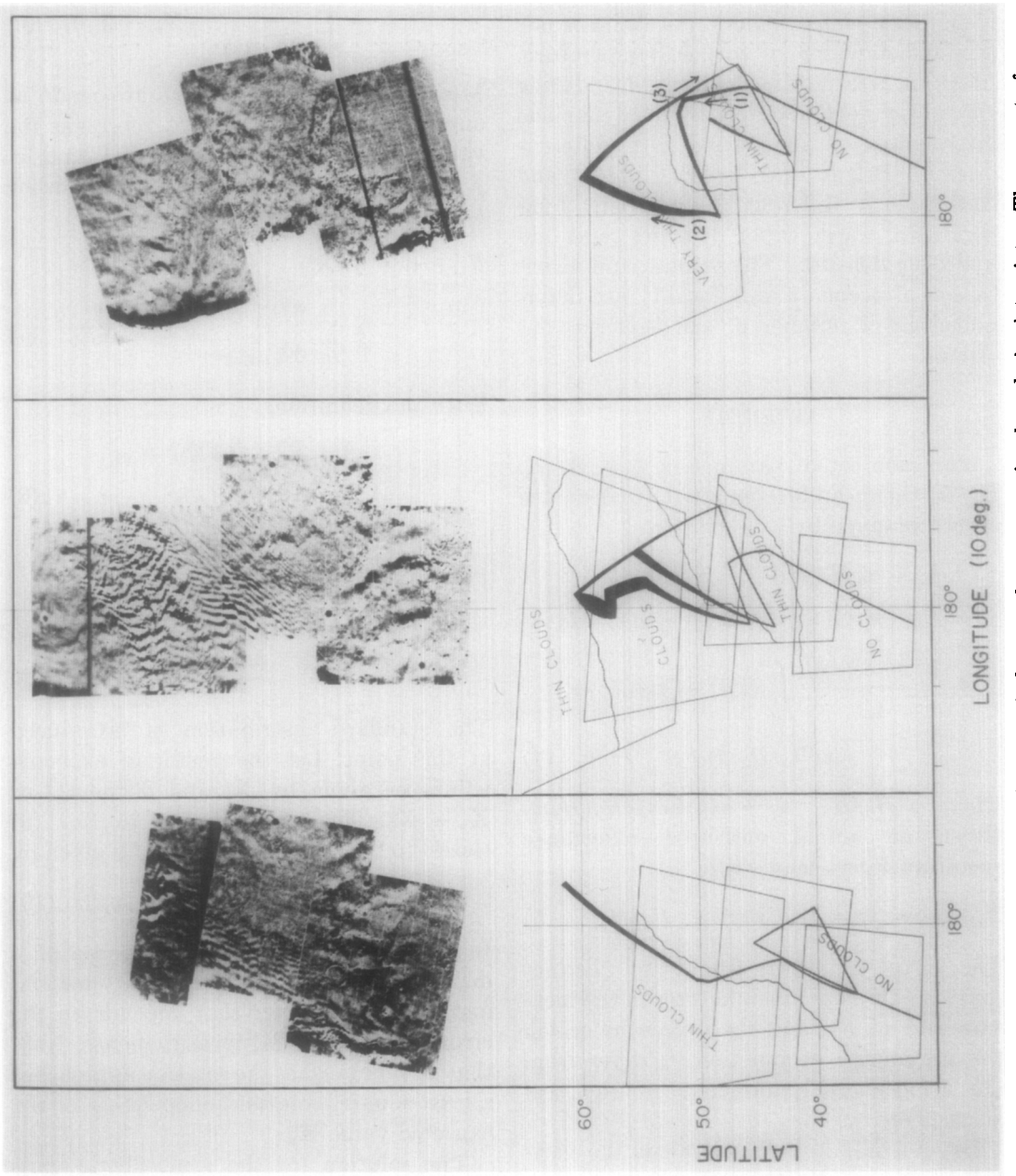

FIG. 9. Photomosaics of a region in the Mars Northern Hemisphere on three consecutive days during late winter. The amount of ozone computed with the homogeneous model is represented by the thickness of the line superimposed onto the rectilinear projection of the TV pictures in the lower portions of the figures (Barth and Dick, 1974).

vapor, is the primary source of odd hydrogen, and the ozone distribution no longer depends on the vertical temperature profile.

A comparison of orbits 202 and 186 demonstrates that the ozone distribution is neither a simple function of latitude nor a simple function of surface temperature. Martian weather in midlatitudes during the spring is characterized by the dynamical interactions of air masses with different origins (Briggs and Leovy, 1974), and consequently different characteristic temperatures, water vapor densities, and odd hydrogen densities. The amount and distribution of ozone at each locality are determined by a number of atmospheric conditions.

APPENDIX

For each set of parameters $\bar{\tau}$, k, A, τ_o, H_o/H_s there can be computed a reflectance spectrum given by

$$f_\lambda(\bar{\tau}, k, A, \tau_o H_o/H_s) = A\mu_0 \exp\{-[\bar{\tau}\beta(k;\lambda) + \tau_o\alpha(\lambda)]M\} + \frac{\bar{\tau}\beta(k;\lambda)p(\psi)}{4\mu}\int_0^1 \exp\{-[\bar{\tau}t\beta(k;\lambda) + \tau_o x(H_o/H_s; t)\alpha(\lambda)]M\}dt, \quad (4)$$

where $x(H_o/H_s;\ t) = \exp\{\ln t/(H_o/H_s)\}$. Given an actual measured reflectance spectrum R_λ we may write

$$R_\lambda + \epsilon_\lambda = f_\lambda = f_\lambda(\bar{\tau}, k, A, \tau_o, H_o/H_s). \quad (5)$$

The error ϵ_λ arises from two distinct sources—the experimental error in the measurement of R_λ, and the degree by which the arguments of function f_λ differ from the atmospheric parameters of the real atmosphere.

Let $X_1, X_2, \ldots, X_5$ represent the variables $\bar{\tau}$, k, $\ldots$, H_o/H_s normalized to order 1 and write $f_\lambda(X_1, X_2, \ldots, X_5)$ as $f_\lambda(\mathbf{X})$. Let $\mathbf{X}^0$ be an initial estimate of the values of the atmospheric parameters. If this initial estimate is sufficiently close to the description of the actual atmosphere, then Eq. (5) may be linearized about it:

$$R_\lambda + \epsilon_\lambda = f_\lambda(\mathbf{X}^0) + \sum_{j=1}^{5} \frac{\partial f_\lambda}{\partial X_j}\bigg|_{\mathbf{X}=\mathbf{X}^0} (X_j - X_j^0). \quad (6)$$

Measurements of reflectance are made at discrete wavelengths. Let R_i represent the values of R_λ for the ith value of λ, and let f_i represent the value of function f_λ when λ takes on its ith value. Then

$$R_i + \epsilon_i = f_i(\mathbf{X}^0) + \sum_{j=1}^{5} \frac{\partial f_i}{\partial X_j}\bigg|_{\mathbf{X}=\mathbf{X}^0} (X_j - X_j^0). \quad (7)$$

With the definitions

$$\begin{aligned} r_i^0 &= R_i - f_i(\mathbf{X}^0) + \epsilon_i, \\ A_{ij}^0 &= \partial f_i/\partial X_j|_{\mathbf{X}=\mathbf{X}^0}, \\ x_j^0 &= X_j - X_j^0, \end{aligned} \quad (8)$$

Eq. (7) is expressed as

$$r_i^0 = \sum_{j=1}^{5} A_{ij}^0 x_j^0. \quad (9)$$

The standard distribution is introduced at this point. Let the vector of expected values be given by $\mathbf{X}_p$ and define $\mathbf{x}_p^0$ as $\mathbf{X}_p - \mathbf{X}^0$. Then the solution to Eq. (9) closest to the standard value $\mathbf{X}_p^0$ is given by

$$\mathbf{x}^0 = (A^{0t}A^0 + \gamma I)^{-1}(A^{0t}\mathbf{r}^0 + \gamma\mathbf{x}_p^0) \quad (10)$$

(e.g., Twomey, 1965). The superscript t denotes transpose, I is the identity matrix, and γ is a parameter that depends on the errors in the spectral measurements. Note that as γ diminishes the solution approaches a least-squares solution independent of the expected value $\mathbf{X}_p$.

The solution for the atmospheric variables is

$$\mathbf{X} = \mathbf{X}^0 + \mathbf{x}^0. \quad (11)$$

However, this solution is based on elements of matrix A^0 that were computed for

atmospheric variables $\mathbf{X}^0$. The solution to this nonlinear set of equations is found by iteration. Let

$$\mathbf{X}^n = \mathbf{X}^{n-1} + \mathbf{x}^{n-1},$$

$$A_{ij}{}^n = \partial f_i/\partial X_j|_{\mathbf{x}=\mathbf{x}^n},$$

$$\mathbf{x}_p{}^n = \mathbf{X}_p - \mathbf{X}^n,$$

and

$$\mathbf{r}^n = \mathbf{R} - \mathbf{f}(\mathbf{X}^n), \qquad (12)$$

where ε is implicitly included in $\mathbf{R}$, and iterate until $\mathbf{X}^{n+1} - \mathbf{X}^n$ is sufficiently small to ensure that $\mathbf{X}$ will not change significantly with further iterations. In order to extract the most information from the spectral measurements, the value of γ chosen is the smallest value for which the iteration process converges.

ACKNOWLEDGMENTS

One of us (W. M. Wehrbein) wishes to express his appreciation to Ian Stewart and Julius London, who, with the coauthors, served on his thesis committee. We wish to thank B. J. Conrath for providing the temperature profiles and Conway Leovy for reading this paper and making many helpful suggestions. This work was supported by the National Aeronautics and Space Administration under Grant NGR 06-003-127.

REFERENCES

Barth, C. A., and Dick, M. L. (1974). Ozone and the polar hood of Mars. *Icarus* **22**, 205–211.

Barth, C. A., and Hord, C. W. (1971). Mariner ultraviolet spectrometer: Topography and polar cap. *Science* **173**, 197–201.

Barth, C. A., Hord, C. W., Stewart, A. I., Lane, A. L., Dick, M. L., and Anderson, G. P. (1973). Mariner 9 ultraviolet spectrometer experiment: Seasonal variations of ozone on Mars. *Science* **179**, 795–796.

Briggs, G. A., and Leovy, C. B. (1974). Mariner 9 observations of the Mars north polar hood. *Bull. Amer. Meteorol. Soc.* **55**, 278–296.

Broida, H. P., Lundell, O. R., Schiff, H. I., and Ketcheson, R. D. (1970). Is ozone trapped in the solid carbon dioxide polar cap of Mars? *Science* **170**, 1402.

Conrath, B. J. (1969). On the estimation of relative humidity profiles from medium resolution infrared spectra obtained from a satellite. *J. Geophys. Res.* **74**, 3347–3361.

Conrath, B., Curran, R., Hanel, R., Kunde, V., Maguire, W., Pearl, J., Pirraglia, J., Welker, J., and Burke, T. (1973). Atmospheric and surface properties of Mars obtained by infrared spectroscopy on Mariner 9. *J. Geophys. Res.* **78**, 4267–4278.

Davis, J. S. (1976). Ozone and water in the lower Martian atmosphere. Master's thesis, Department of Astro-Geophysics, University of Colorado at Boulder.

Hord, C. W., Barth, C. A., and Pearce, J. B. (1970). Ultraviolet spectroscopy experiment for Mariner Mars 1971. *Icarus* **12**, 63–71.

Hord, C. W., Simmons, K. E., and McLaughlin, L. K. (1974). Mariner 9 ultraviolet spectrometer experiment: Pressure–altitude measurements on Mars. *Icarus* **21**, 292–302.

Lane, A. L., Barth, C. A., Hord, C. W., and Stewart, A. I. (1973). Mariner 9 ultraviolet spectrometer experiment: Observations of ozone on Mars. *Icarus* **18**, 102–108.

Mateer, C. S. (1965). On the information content of Umkehr observations. *J. Atmos. Sci.* **22**, 370–381.

McElroy, M. B., and Donahue, T. M. (1972). Stability of the Martian atmosphere. *Science* **177**, 986–988.

Parkinson, T. D., and Hunten, D. M. (1972). Spectroscopy and aeronomy of O_2 on Mars. *J. Atmos. Sci.* **29**, 1380–1390.

Twomey, S. (1963). On the numerical solution of Fredholm integral equations of the first kind by the inversion of the linear system produced by quadrature. *J. Assoc. Comput. Mach.* **10**, 97–101.

Twomey, S. (1965). The application of numerical filtering in the solution of integral equations encountered in indirect sensing measurements. *J. Franklin Inst.* **279**, 95–109.

Wehrbein, W. M. (1977). Description of the vertical distribution of ozone in the Martian atmosphere from Mariner 9 ultraviolet spectrometer data. Ph.D. thesis, Department of Astro-Geophysics, University of Colorado at Boulder.